ACS Sustainable Chemistry & Engineering

Research Article

pubs.acs.org/journal/ascecg

Sustainable Materials: Value-Added Composites from Recycled Polypropylene and Fly Ash Using a Green Coupling Agent

Shubhalakshmi Sengupta,[†] Dipa Ray,[†,*] and Aniruddha Mukhopadhyay[‡]

[†]Department of Polymer Science and Technology, University of Calcutta, 92, A.P.C. Road, Kolkata-700009, India

[‡]Department of Environmental Science, University of Calcutta, 35, Ballygunge Circular Road, Kolkata-700019, India

ABSTRACT: Composites were developed from two industrial wastes: recycled polypropylene (R) and fly ash (FA). Surface coating of fly ash (FA) particles with palmitic acid (PA) in different wt % of 1, 2, 3, and 5 were done, and they were incorporated as filler in the R matrix by melt mixing. X-ray diffraction analysis (XRD), mechanical characterization, dynamic mechanical analysis (DMA), differential scanning calorimetry (DSC), thermogravimetric analysis (TGA), and fracture surface analysis were carried out with a scanning electron microscope (SEM) to establish structure−property correlation. Crystallinity changed significantly, resulting in improved properties in 1 wt % PA-coated FA/R (RFAPA1) and 2 wt % PA-coated FA/R (RFAPA2) composites. Impact strength increased by 132% in RFAPA1, and an increase in glass transition temperature was observed in RFAPA1 and RFAPA2. RFAPA1 and RFAPA2 exhibited enhanced thermal stability, and SEM revealed improved interfacial compatibility. These results showed the possibility of using a renewable green chemical like PA as a coupling agent in place of conventional expensive silane coupling agents to develop sustainable value-added polymer composites from environmentally hazardous waste materials.

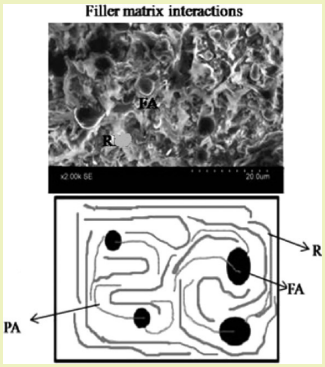

KEYWORDS: *Green composites, Recycling, Surface treatments, Particle reinforcement, Thermal properties*

INTRODUCTION

Today's world is moving toward the development of sustainable materials that are both economically viable and environmentally friendly. In this aim, development of value-added materials from recycled industrial waste like polypropylene (PP) and fly ash (FA) is an interesting approach.[1] Plastic wastes like that of polypropylene take a lifetime for degradation, so recycling of the polymers and production of new materials with good properties is desired.[1,2] Again, fly ashes are byproducts of thermal power plants and constitute about 85% of the total residue generated from the coal combustion process having harmful environmental effects such as air pollution and groundwater contamination due to leaching of metals from them when disposed openly in the environment.[2,3] The composition of fly ash vary depending upon the source of coal and is comprised primarily of SiO_2 along with lower contents of Al_2O_3, Fe_2O_3, Na_2O, MgO, K_2O, etc.[4,5] Nowadays, attempts are being made to establish fly ash as attractive mineral filler in various polymer matrix composites having different engineering applications,[4,6−8] which would enable their removal from the environment and their effective use. Gupta et al. reported that the addition of fly ash particles lowered the compressive strength of glass fiber/epoxy composites, but the impact strength increased considerably.[9] Menon et al. reported the use of fly ash as a filler in natural rubber in the presence of 5−10 phr of phosphorylated cardanol prepolymer (PCP) and hexamethylenetetramine cured PCPthat resulted in higher thermal stability along with improvement in mechanical properties.[10] Sridhar et al. reported an initial increase in tensile properties with a subsequent drop in properties with an increase in fly ash loadings. They also reported an increase in thermal stability with increasing fly ash content in fly ash/waste tire powder/isotactic PP composites.[7] Ray et al. studied the changes in the mechanical properties of the vinylester resin matrix composites that were fabricated with 30, 40, 50, and 60 wt % fly ash loadings by a room temperature casting method. The study reported that fly ash can be used effectively to increase the rigidity and stiffness of the vinyl ester resin matrix; however, there was a lowering in the property above 50 wt % of fly ash loading.[5] In a separate study, these composites showed faster thermal degradation at a lower temperature in the case of the 30 and 60 wt % composites and a higher onset temperature for the 40 and 50 wt % composites.[11]

However, according to Yu-fen et al., improvement of composite strength by using fly ash as a filler has problems regarding the weak interfacial bonding between untreated fly ash and polymer due to low friction of the fly ash surface. So, a modification of fly ash was done by various techniques where either coupling agents or surfactants were used followed by mechanical mixing.[12] Bose et al. in their study concluded that the usage of a coupling agent played a significant role in improving the mechanical properties of fly ash/nylon 6 composites.[13] Nath et al. reported that sodium lauryl sulfate (SLS)-treated fly ash/polyvinyl alcohol (PVA) composites

Received: September 10, 2012
Revised: April 24, 2013
Published: April 30, 2013

   dx.doi.org/10.1021/sc3000948 | ACS Sustainable Chem. Eng. 2013, 1, 574−584

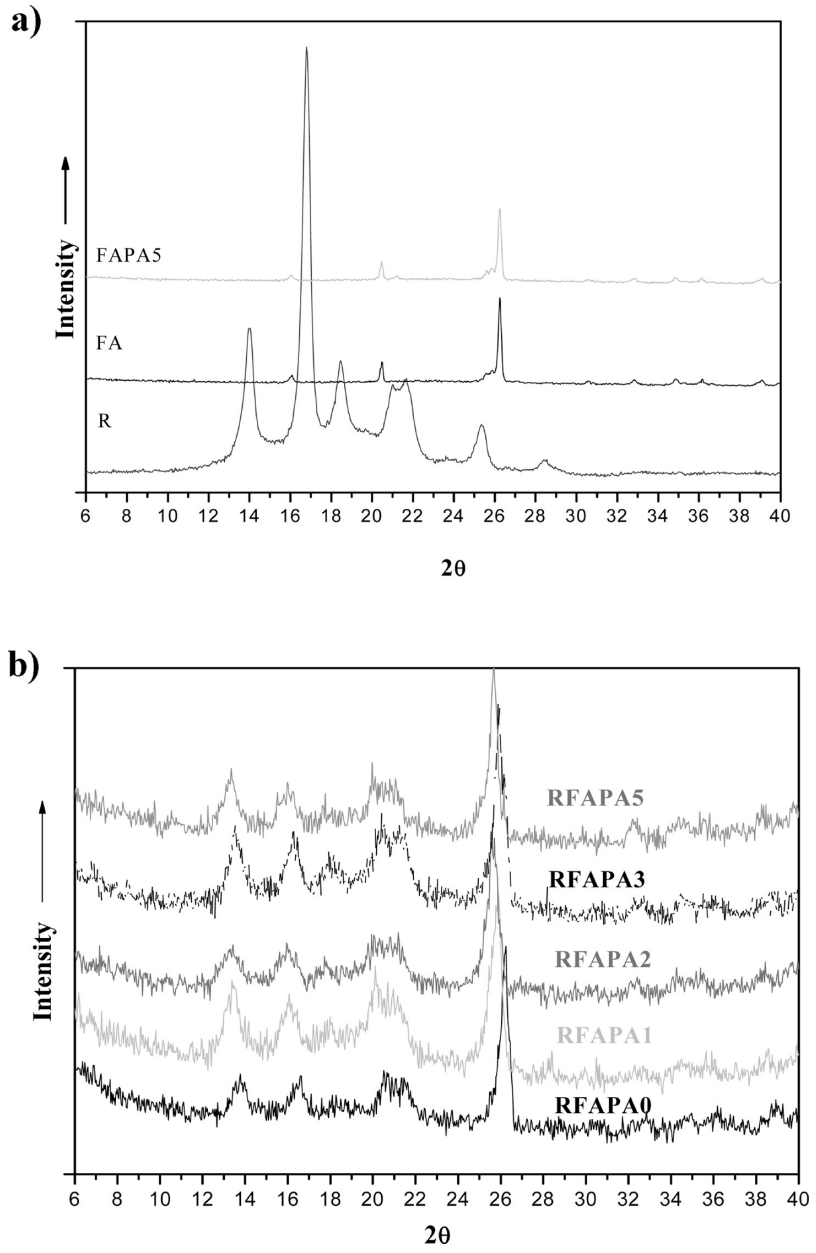

Figure 1. XRD analysis of (a) R, FA, and FAPA5 and (b) composite samples.

showed a 33% higher strength than untreated fly ash/PVA composites. This increase in strength was attributed to the level of physical bonding between SLS-FA and PVA surfaces.[14] Pardo et al.[4] reported that improved stiffness and strength of materials were observed when silane coupling agents of three types containing different reactive functional groups like amine (GF96), vinyl (XL10), and vinyl-benzylamine (Z-6032) were used in mixing fly ash with isotactic polypropylene matrix along with improved thermal stability. This improvement was greater in the composites containing vinyl and amino silane-treated fly ashes, which showed a higher onset temperature that was strongly dependent on filler−matrix adhesion.[4] Das et al. reported the utilization of recycled polypropylene by forming composites with fly ash in a 1:1 weight ratio using two types of coupling agents (vinyl trimethoxy silane coupling agent, VTMO and maleated polypropylene, Epolene G3003). Thermal stability was found to be much higher in the VTMO-treated composites compared to the untreated ones, which was the result of enhanced interaction at the matrix−filler interface in the presence of the coupling agent VTMO.[15]

In our earlier study, the mechanical properties of furfuryl palmitate (FP)-coated fly ash-reinforced recycled polypropylene matrix composites were reported by us.[16] The highest enhancement in mechanical properties was observed in 2 wt % FP-coated fly ash-filled composites, and the highest impact strength was observed in 1 wt % FP-coated fly ash-filled composites. A renewable chemical like furfuryl palmitate was seen to be an effective coupling agent for fly ash for the first time in place of expensive silane coupling agents that are more commonly used.[16]

In this study, palmitic acid (PA) was used as a coupling agent between the fly ash particles and recycled polypropylene matrix. The efficacy of a nonconventional green coupling agent like PA in a FA/R composite system, where filler and matrix are present in equal proportion, was investigated in this study. Detailed

dx.doi.org/10.1021/sc3000948 | ACS Sustainable Chem. Eng. 2013, 1, 574−584

mechanical, thermal, and structural characterizations of the composites were done.

MATERIALS AND METHODS

Materials. Fly ash used was collected from the Kolaghat Thermal Power Station, India. This ASTM class "F" fly ash (as per ASTM-C 618) was found to have different proportions of oxides (59% SiO_2, 21% Al_2O_3, 8% Fe_2O_3, and the rest other oxides).[11] The ash particles had the following particle size distribution: 10% of the samples had a particle size below 2.38 μm, 50% of the samples had particle sizes below 13.58 μm, and 90% of the samples were below 111.16 μm. Recycled polypropylene (R) was obtained from recycled post-consumer plastic products and was used as the matrix material. Palmitic acid and the solvents acetone and toluene were obtained from Loba Chemie Pvt. Ltd., Mumbai, India.

Surface Treatment of Fly Ash and Fabrication of Composites. The fly ash particles (50 g) were immersed in a 100 mL solution of palmitic acid (PA was dissolved in a solvent blend of acetone and toluene in the ratio of 3:1 by volume) followed by stirring for 15 min. Four separate sets of coated fly ash particles were prepared with 1, 2, 3, and 5 wt % PA, and each set was replicated twice. They were kept for drying for 2 days at room temperature and then vacuum dried to completely remove the solvents. The surface-coated fly ash particles were designated as FASAX, where X denoted the wt % of PA with respect to the weight of fly ash coated. The surface-coated fly ash (FASAX) particles and the recycled polypropylene (R) were taken in a 1:1 weight ratio and were mixed in an internal mixer (Brabender 30/50 E, Germany) for 20 min at a temperature of 170 °C. A similar set was also prepared with uncoated fly ash particles (FAPA0) and recycled polypropylene matrix laminates (R). The resultant melt mixed compound was compression molded at 170 °C to form the composite laminates. The composites were designated as RFAPA0, RFAPA1, RFAPA2, RFAPA3, and RFAPA5, and the unreinforced laminate as R. The surface coating of FA and fabrication of the composites technique was done according to our earlier reported study[16] along with some modifications.

X-ray Diffraction Analysis. XRD analysis was done using X-ray diffractometer X Pert Pro (PANalytical, Almelo, The Netherlands) with Cu Kα radiation operating at 40 kV and 30 mA at a scanning rate of 2° min^{-1} in the range of diffraction angle 2θ = 5−90°.[17] The surface-coated fly ash particles (FA, FAPA1, and FAPA5), R, and the composites were analyzed.

Flexural and Impact Testing. The composite samples were tested for their flexural properties under three point bending in an Instron 4303 (Norwood, MA, U.S.A) in accordance with ASTM D790-10.[17] Five samples of each set were tested to get the mean value, and the standard deviation was also reported. In the case of matrix R, the flexural properties were also studied. Flexural strength and flexural modulus were studied up to 5% strain for R.[18]

Impact strengths of the samples were tested in a CEAST Izod (WinPEN CEAST S.p.A, Turin, Italy) impact tester following ASTM D 256-10.[19] Five samples of each set in both flexural and impact testing were tested to get the mean value, and the standard deviation was also calculated. The statistical analysis was done using Origin 8 software (OriginLab Corporation, Northampton, U.S.A.), and all the graphs of this study were plotted using the same. The test values were also statistically analyzed (paired t test) between the uncoated FA/R (RFAPA0) composites and the PA-coated FA/R composites (RFAPA1, RFAPA2, RFAPA3, and RFAPA5) in order to determine whether the differences incurred were statistically significant by employing Minitab 13 software (Minitab, Inc., State College, PA, U.S.A.).

Dynamic Mechanical Analysis (DMA). Dynamic mechanical analysis of the composite samples was carried out with DM Q 800, (TA Instruments, New Castle, DE, U.S.A.) in a nitrogen atmosphere in a three point bend mode at a fixed frequency of 1.0 Hz. The samples were evaluated in the temperature range from −50 to 150 °C with a heating rate of 10 °C per minute.[7,16]

Thermogravimetric Analysis (TGA). The thermal degradation behavior was studied in a TGA Q 50 V 20 Build 36, Universal V4 5A (TA Instruments, New Castle,DE, U.S.A.). The samples (5−10 mg) were scanned from 25 to 600 °C at a heating rate of 10 °C/min in nitrogen environment.[7,20]

Differential Scanning Calorimetry (DSC). DSC analysis of the composite samples (5−10 mg) was done using a DSC Q20 V 24.4 Build 116 (TA Instruments, New Castle, DE, USA) at a heating rate of 10 °C/min in the temperature range between −50 and 200 °C in a nitrogen environment. The cooling and second heating were then done at the same rate to evaluate the thermal transition behavior of the composites.[17,20]

The graphs for XRD, DMA, TGA, and DSC analysis were plotted using Origin 8 software (OriginLab Corporation, Northampton, MA, U.S.A.).

Scanning Electron Microscopy (SEM). The fracture surface of the composite samples were coated with a Au−Pd alloy and investigated under SEM (Hitachi S-3400N, Krefeld, Germany).

RESULTS AND DISCUSSION

The structural, mechanical, and thermal properties of palmitic acid-coated fly ash-reinforced recycled polypropylene matrix composites were extensively studied in order to evaluate their efficiency as novel composite material with potential application possibilities.

X-ray Diffraction Analysis. To find out the structural changes incurred by the composite in the presence of the coupling agent PA, XRD analysis was carried out. The X-ray diffractograms of R, FA, and FAPA5 are shown in Figure 1a and of the composites (RFAPA0, RFAPA1, RFAPA2, RFAPA3, and RFAPA5) in Figure 1b. The % crystallinity and the crystallite size of R and of R in the composites were calculated and given in Table 1. The crystallite size was calculated using the Scherrer's equation

$$L_{h,k,l} = K\lambda/\beta\cos\theta$$

where K = 0.94, β is the full width half maxima perpendicular to each plane, and θ is Bragg's angle.[21] The % crystallinity was calculated per the formula

Table 1. % Crystallinity and Crystallite Size of R, RFAPA0, RFAPA1, RFAPA2, RFAPA3, and RFAPA5

	peak position (2θ)	% crystallinity	crystallite size (nm)
R	13.9	80	52.5
	16.8	95	47.1
	18.4	65	52.1
	20.9	65	47.1
	21.6	68	37.2
RFAPA0	13.7	80	21.4
	16.5	81	21.5
	20.6	84	10.8
RFAPA1	13.9	82	32.3
	16.7	80	25.9
	20.7	70.6	51
RFAPA2	13.9	83.6	16.1
	16.6	86.4	21.5
	20.7	70.4	9.2
RFAPA3	13.9	76.2	32.2
	16.6	75.5	25.8
	21.7	60	10.8
RFAPA5	13.86	82.8	32.2
	16.62	79.9	18.4
	20.85	70	10.83

dx.doi.org/10.1021/sc3000948 | ACS Sustainable Chem. Eng. 2013, 1, 574−584

$$\% \text{ Crystallinity} = (I_{h,k,l} - I_{amp})/I_{h,k,l} \times 100$$

for each crystalline plane of the matrix,[21] $I_{h,k,l}$ corresponds to the maximum intensity of the particular α monoclinic planes of either (110), (040), (130), (111), or (131), respectively, and I_{amp} corresponds to the intensity of the amorphous region. The calculated % crystallinity and crystallite size values are given in Table 1.

In Figure 1a, R showed a diffraction pattern similar to a semicrystalline polymer with sharp peaks and an amorphous halo underneath. The Bragg reflections were observed at around 2θ = 14.1°, 16.8°, 18.5°, 21°, and 22°, respectively, which were similar to that of polypropylene, and these positions corresponded to the indexed planes of α monoclinic planes of (110), (040), (130), (111), and (131), respectively.[17,22] The characteristic peaks of fly ash, both in surface coated and uncoated forms, were observed at 2θ = 26.6°. In the composites, a reduction in peak intensity and sharpness was evident as a result of lessening in the amount of the polymer matrix. Incorporation of the crystalline fly ashes was also evident. However, surface coating of fly ashes and their incorporation into the matrix resulted in changes in the crystalline nature of the polymer. The change in polymer crystallinity due to incorporation of FA cenospheres in the PP matrix was also reported earlier.[23]

The composites showed the characteristic peaks of the monoclinic (110), (040), and (111) planes. In the composites, only 50% R was present, so a decrease in both the noncrystalline and crystalline portions had occurred that resulted in reduction of the peak intensities, as evident in Figure 1b. Among all the PA-treated composites, the highest increase in % crystallinity and crystallite size was observed in the case of RFAPA2, followed by RFAPA1and RFAPA5. The highest increase in % crystallinity was observed in the (040) plane of RFAPA2. A significant reduction of the crystallite size in PA-coated FA/R composites was also observed, especially in the case of RFAPA2. Reduction in crystallite size in the presence of heterogeneous nucleating agents in polypropylene has been reported earlier.[24] So, PA coated fly ash might have acted as an efficient nucleating agent in altering the crystallization properties of R.

Thus, from XRD analysis, it could be viewed that filler–matrix interaction in the presence of the coupling agent changed the molecular packing order and the crystallization characteristics of the composites. Whether these changes resulted in enhancement of mechanical and thermal properties of the composites was further evaluated.

3.2. Flexural and Impact Testing. The variations of the flexural strength, modulus, and strain of the matrix (R) and the composites (RFAPA0, RFAPA1, RFAPA2, RFAPA3 and RFAPA5) are given in Figure 2a–c. It was observed from Figure 2a that the flexural strength decreased on addition of fly ash by 68% in RFAPA0 in comparison to that of R. A decrease in flexural strength on incorporation of filler in the polymer matrix has been reported earlier.[25] Incorporation of filler by 50 wt % in the R matrix reduced the polymer chain entanglements as fly ash particles entered between the R chains. In PA-coated FA/R composites, the flexural strength increased by 12% in RFAPA1 and by 46% in RFAPA2 with respect to RFAPA0. This increase may be attributed to the enhanced stress transfer at the interface between coated fly ash particles and the R matrix owing to better entanglement between PA chain moieties and R chains.[16] In the case of RFAPA3 and

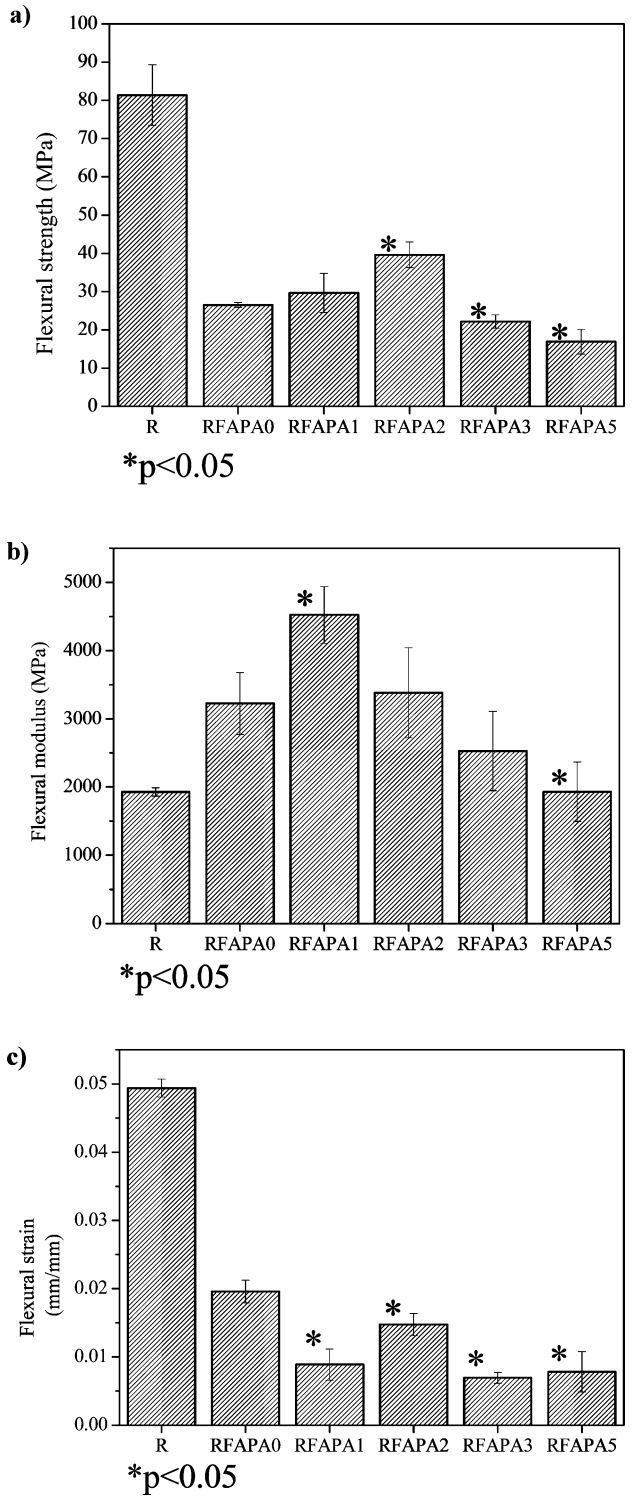

Figure 2. Variation in (a) flexural strength, (b) flexural modulus, (c) strain of R, and the composite samples.

RFAPA5, there was a reduction in flexural strength in comparison to RFAPA0 by 16% and 36%, respectively. This could be due to increased smoothening of fly ash surfaces resulting in lower stress transfer at these higher concentrations of palmitic acid.

The presence of fly ash and PA-coated fly ash particles increased the rigidity of the composites. The modulus values of RFAPA0 increased by 67% from that of R. Incorporation of

filler increases the flexural modulus due to a restriction in chain mobility when the load is applied on the composite. Such an increase in flexural modulus with a decrease in flexural strength in polypropylene on incorporation of filler was reported earlier.[26] The modulus values also increased by 40% and 5% in RFAPA1 and RFAPA2, respectively, and decreased by 28% and 40% in RFAPA3 and RFAPA5, respectively, compared to that of RFAPA0. Thus, RFAPA1 and RFAPA2 showed enhancement in mechanical properties among the composites.

The strain values of RFAPA1, RFAPA2, RFAPA3, and RFAPA5 decreased by 55%, 25%, 64%, and 60%, respectively, in comparison to the value of RFAPA0. As discussed earlier, the presence of a coupling agent influenced the interfacial bonding and influenced the mechanical properties of the composites. Use of a silane coupling agent in a fly ash/recycled polypropylene matrix was studied earlier where it was reported that a 6 wt % Dynasylan VTMO-treated composite showed an increase of 4% and 15% in flexural strength and modulus, respectively, in comparison with the untreated ones.[15] Thus, palmitic acid played an efficient role as a coupling agent when compared with a conventionally used silane coupling agent. Palmitic acid as a coupling agent also showed higher enhancement in flexural strength and modulus values when compared to furfuryl palmitate, which was studied in our previous work.[16]

The impact strengths of R and the composites were also studied (Figure 3). Impact strength decreased in RFAPA0 from

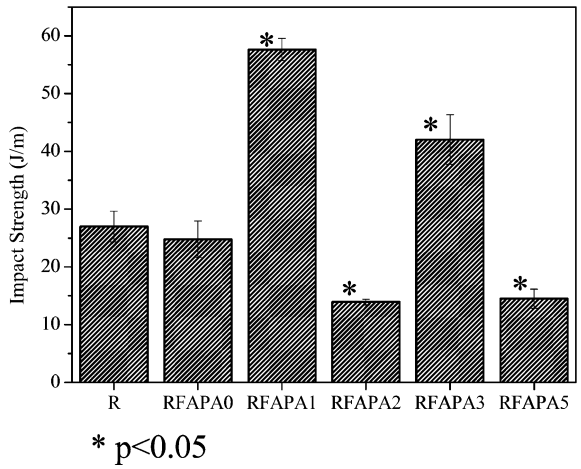

Figure 3. Variation in impact strength of R and the composite samples.

R by 8%. Among the composites, RFAPA1 and RFAPA3 showed an increase of impact strength by 132% and 70% when compared to that of RFAPA0 and decreased by 44% and 43% in RFAPA2 and RFAPA5, respectively. In our earlier study, 2 wt % furfuryl palmitae-coated FA/R composites also showed a decrease in impact strength, whereas its flexural strength was highest among the composites.[16]Thus, palmitic acid aided in enhancing the impact strength of the above-mentioned two composites. This observation indicates that the alignment of the R molecules in the presence of PA at the interface lead to different crystalline arrangements, and the impact strength was influenced accordingly.

Dynamic Mechanical Analysis (DMA). The dynamic mechanical analysis of R and the composite samples was carried out to investigate the properties of the composites under dynamic loading conditions with an increase in temperature. The variation of the storage modulus as a function of temperature is shown in Figure 4a. The storage modulus of all the composites increased from that of R with RFAPA1 showing the highest value. The variation of loss modulus as a function of temperature is shown in Figure 4b. The loss modulus of all the composites increased with respect to R, but among the composites, surface-coated FA-filled composites had lower loss modulus values than RFAPA0, with RFAPA2 being the least. The glass transition temperatures (T_g) measured from the main peak of the loss modulus curves were 12.4, −1.6, +5.3, +5.6, −2.8, and −0.9 °C for R, RFAPA0, RFAPA1, RFAPA2, RFAPA3, and RFAPA5, respectively. The shift from a glassy to rubbery state occurred at a lower temperature in RFAPA0 than that of R as the incorporation of filler influenced the molecular mobility. A delayed transition from a glassy to rubbery state was witnessed in RFAPA1 and RFAPA2 with respect to RFAPA0, indicating a restricted mobility of the molecules in the amorphous fraction. The different crystalline fractions formed in the samples influenced the mobility of the amorphous chains. All the surface-coated FA-filled composites showed a small second loss modulus peak at higher temperatures of 76, 81, 80, and 76 °C in RFAPA1, RFAPA2, RFAPA3, and RFAPA5, respectively, but not in the R and RFAPA0 samples. The appearance of two loss modulus peaks at a lower and a higher temperature might be attributed to the mobility of the polymer molecules in the bulk and near the interface, respectively. This type of loss modulus spectra was reported earlier in the case of kenaf fiber-filled polypropylene composites where two transitions were seen due to relaxation of unrestricted PP chains and restricted PP chains at lower and higher temperatures, respectively.[27] This also clearly indicated that the presence of PA at the interface significantly influenced the interfacial bonding that restricted the mobility of the R molecules near the interface and showed a delayed transition from glassy to rubbery state.

The variation of the damping parameter (tan δ) as a function of temperature is shown in Figure 4c. The PA-coated FA/R composites showed reduction in the damping (tan δ) values with respect to RFAPA0. The damping (tan δ) values of R, RFAPA0, RFAPA1, RFAPA2, RFAPA3, and RFAPA5 at the transition temperature were 0.084, 0.098, 0.077, 0.067, 0.078, and 0.074, respectively.

Thus, from the increase in the storage modulus values and the shift in the *T*g values to a higher temperature in the PA-coated FA/R composites, it could be inferred that an improvement in interfacial bonding occurred in PA-treated composites particularly in the case of RFAPA1 and RFAPA2, and this is fully corroborated with the flexural test observations.

Thermogravimetric Analysis (TGA). Thermal stability of the composites was studied through TG analysis. The TGA graphs of composite samples, i.e., weight change of the composites with respect to temperature, are depicted in Figure 5a. It was observed from Figure 5a that the onset of degradation occurred at 280 °C in R. The TGA thermogram of only FA is shown in the inset, where fly ash being a noncombustible material did not show any weight loss. On incorporation of filler FA in the polymer matrix, the degree of entanglement between the polymer chains was altered, resulting in a continuous change of weight ranging between 250 and 450 °C. In the cases of RFAPA0, RFAPA1, and RFAPA2, the onset of degradation ranged between 300 and 400 °C, whereas in RFAPA3 and RFAPA5, it appeared at 375 and 360 °C,

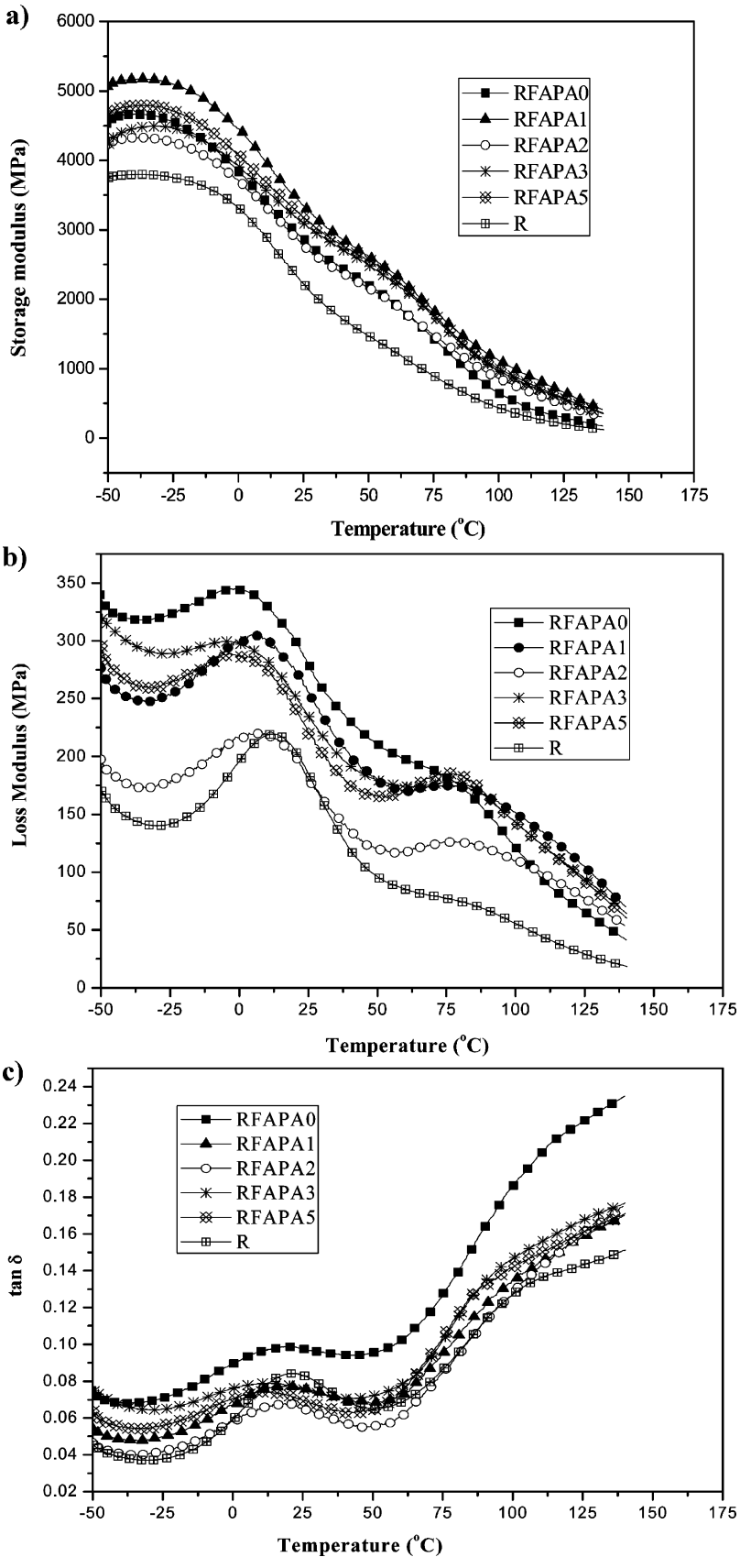

Figure 4. Variation of (a) storage modulus, (b) loss modulus, and (c) tan δ of R and the composite samples.

respectively. To evaluate the weight loss of the composite samples on thermal degradation, average weight loss of the composites and the R laminate in an ascertained temperature range was calculated from the TGA data (Table 2). This type of

dx.doi.org/10.1021/sc3000948 | ACS Sustainable Chem. Eng. 2013, 1, 574−584

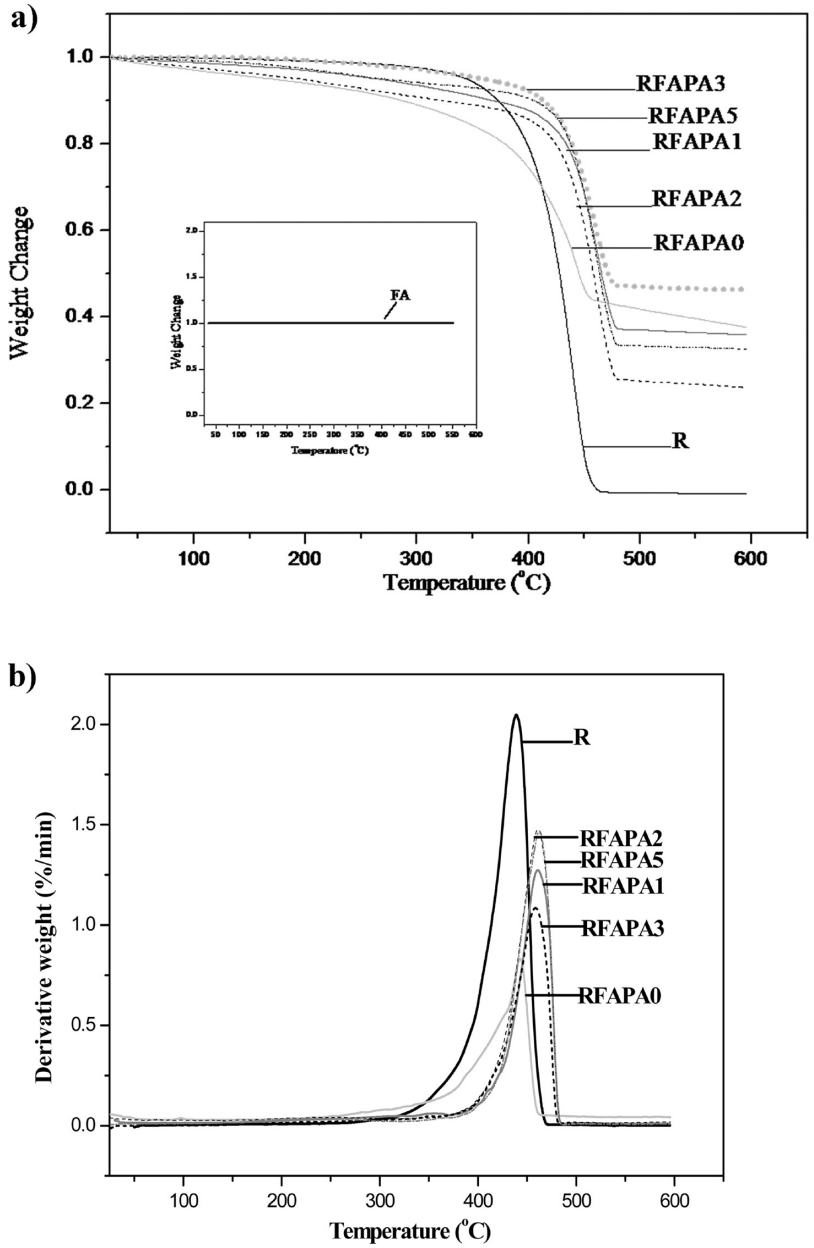

Figure 5. (a) TGA plot of R and the composites (plot of TGA of FA in the inset). (b) DTGA plots of R and the composite samples.

Table 2. Average Weight Loss of R and the Composites in Different Temperature Ranges (derived from TGA data)

temperature range	R	RFAPA0	RFAPA1	RFAPA2	RFAPA3	RFAPA5
250−300 °C	1%	9%	5%	8%	3%	5%
300−350 °C	5%	13%	8%	10%	4%	6%
350−400 °C	11%	20%	10%	12%	6%	8%
400−450 °C	51%	39%	19%	22%	15%	17%

representation of the TGA data revealed that in the case of R, the degradation occurred at one point, and the degradation was very fast as it encountered a 50% weight loss in the temperature range from 400 to 450 °C, but on incorporation of filler, this pattern changed. The onset of thermal degradation started at an earlier temperature, as in 300−350 °C, the weight loss in RFAPA0 was 13% compared to 5% of R. This early onset of thermal degradation at RFAPA0 could be a result of changes in the degree of entanglement of the polymer chains due to incorporation of the filler. But in the presence of the PA coupling agent, the weight loss in the temperature range of 300−350 and 350−400 °C was reduced further in all the PA-coated FA/R composites when compared to RFAPA0. Thus, it was evident that improved interfacial bonding and reorientation of the chains enhanced the thermal stability of the composites, which corroborated earlier results of structural and mechanical properties. It was observed from Figure 5a and Table 2 that RFAPA1, RFAPA2, RFAPA3, and RFAPA5 were thermally more stable than RFAPA0 and R. In Figure 5b, the DTGA curves showed a similar pattern for the rate of degradation. The

dx.doi.org/10.1021/sc3000948 | ACS Sustainable Chem. Eng. 2013, 1, 574−584

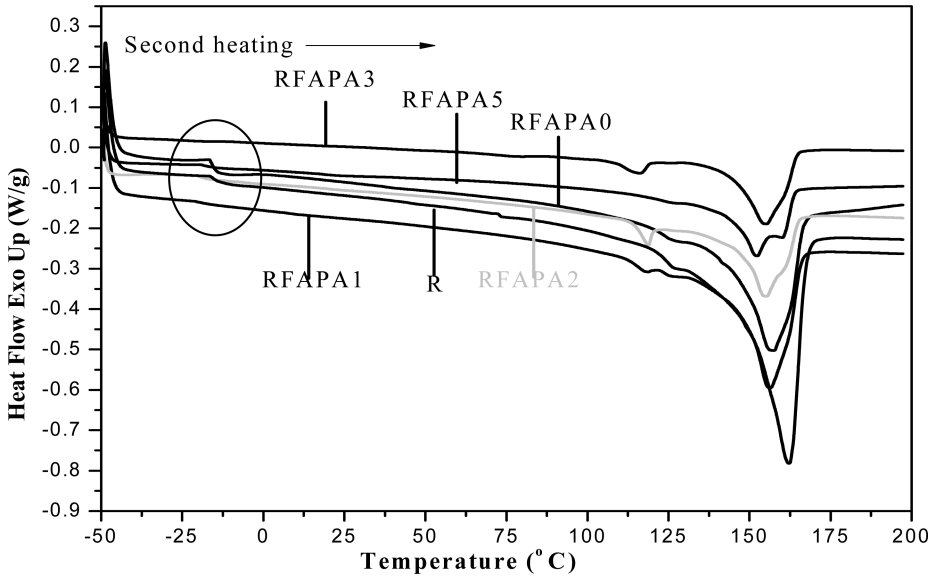

Figure 6. DSC plot of the second heating cycle of R and the composite samples.

Table 3. T_c, T_m, and Enthalpies (ΔH) of the Composites during DSC Cooling and Second Heating Cycles

	DSC cooling cycle		DSC second heating cycle	
composite samples	T_c (°C) (melt crystallization temperature from cooling cycle)	ΔH_c (J/g) (crystallization enthalpy)	T_m (°C) (melting temperature from second heating cycle) Peak 1, Peak 2	ΔH_m (J/g) (melting enthalpy corresponding to Peak 1)
R	122.7	86.7	162.2	56.9
RFAPA0	113.5	55.1	157.3	45.4
RFAPA1	115.4	44.4	156.6	30.3
RFAPA2	115.6	24.8	105, 155.1	14.8
RFAPA3	116.1	20.8	108.9, 155.4	14.0
RFAPA5	114.8	23.3	152.5	16.3

highest rate of degradation of R, RFAPA0, RFAPA1, RFAPA2, RFAPA3, and RFAPA5 were observed at 438, 443, 461, 461, 458, and 463 °C, respectively. The highest degradation peak thus shifted to a higher temperature in the PA-coated FA/R composites. Thus, incorporation of filler improved the thermal stability, and in the presence of the coupling agent, strong filler−matrix interaction was prevalent. From overall results and from the DTGA curves, it could be said that all the PA-coated FA/R composites had more enhanced thermal stability than R and RFAPA0.

Differential Scanning Calorimetry (DSC). The DSC curves of the composites are given in Figure 6. The melt crystallization temperature (T_c), crystallization enthalpy (ΔH_c) obtained from the cooling cycle, and the melting point (T_m) and melting enthalpy (ΔH_m) values obtained from the second heating cycle are given in Table 3. The R matrix showed slightly higher single melting peaks and cooling peaks with higher enthalpy values than the composites. In RFAPA0, a single sharp peak (T_m) was observed at 157 °C along with a distinct T_g at −16 °C and an endothermic peak at 126 °C (Figure 6). In the case of the PA-treated FA/R composites, single melting peaks were observed with RFAPA1 showing the highest melting peak among them. In the case of RFAPA2 and RFAPA, small but prominent peaks at 105 and 109 °C were witnessed, respectively. The presence of multiple melting peaks could be related to the occurrence of several crystallographic forms of PP that were reported earlier .[24] Highly prominent and distinct glass transition temperatures (T_g) were observed in R and RFAPA0 as shown in Figure 6, whereas in all PA-coated FA/R composites, a sharp transition at T_g was not observed, and the transitions were much less pronounced than those observed for R and RFAPA0. A distinct presence of T_g is a result of the clear mobility of the amorphous chains as observed in the case of R and RFAPA0. In composites with surface-coated fly ashes, reduction in the amorphous region might have occurred with an increase in the crystalline portion due to reorientation of the R molecules showing a distinct change in the T_g pattern. This corroborated well with the XRD observations. Thus, incorporation of PA-coated filler lead to changes in the crystalline morphology of the composites influencing their thermal and mechanical properties.

The melt crystallization peak temperature during the cooling cycle (T_c) decreased in RFAPA0 (113 °C) from that of R (122 °C) but increased in PA-coated FA/R composites ranging between 115 and 116 °C, exhibiting the ease of crystallization in the presence of the PA coupling agent. The RFAPA1 showed the highest exothermic ΔH_c value during melt crystallization compared to other treated composites. RFAPA1 also showed the highest melting enthalpy ΔH_m value followed by RFAPA2, indicating the highest crystallinity among these treated composites, and this supported the XRD results. Thus, palmitic acid as a coupling agent was found to influence the structural properties of R/FA composites significantly with distinct indications of polymer chain reorientation.

Scanning Electron Microscopy (SEM). From the structural, mechanica, and thermal properties studied so far in

dx.doi.org/10.1021/sc3000948 | ACS Sustainable Chem. Eng. 2013, 1, 574−584

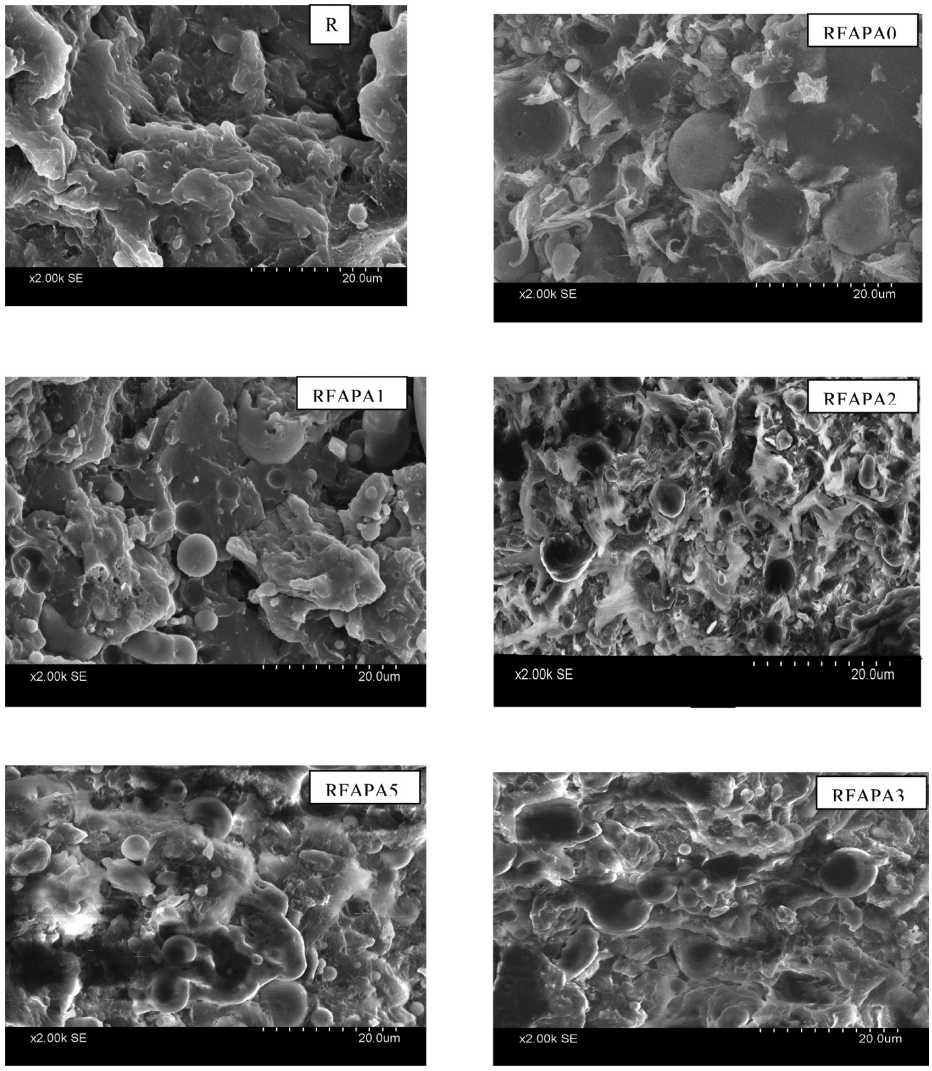

Figure 7. SEM micrograph of composite samples R, RFAPA0, RFAPA1, RFAPA2, RFAPA3, and RFAPA5.

the composites, the presence of the coupling agent (PA) resulted in significant changes in the properties of the composites that can be attributed to the efficient filler matrix interaction of R and FA. To clearly visualize this interaction, the fractured surfaces were investigated under SEM (Figure 7). In RFAPA0, a weak filler−matrix interface was visible. In RFAPA1, this interaction improved with better incorporation of filler within the R matrix. RFAPA2 showed good filler−matrix interaction with ductile failure of the matrix. This supports the high strain value of the composite among PA-coated FA/R composites. In both RFAPA3 and RFAPA5, enhanced wetting of the fly ash by the matrix R was visible. This filler−matrix interaction in the presence of the coupling agent was discussed in our earlier work.[16] In this case, it could also be said that the hydrophilic ends of the long chain palmitic acid might have interacted with the fly ash particles, and their long hydrophobic chains might have formed compatible interfaces with the polymer. However, the extent of entanglement between the palmitic acid molecules and the R chains and the amount of palmitic acid present at the interface controlled the extent of compatible interface produced or resulted into an agglomeration effect. A schematic representation of a possible physical interaction leading to interfacial compatibilization between the filler and matrix in presence of the palmitic acid is shown in Figure 8.

CONCLUSIONS

The PA-coated FA/R composites were evaluated for their structural, mechanical, and thermal properties. The structural analysis (XRD) revealed that the filler−matrix interaction in the presence of the coupling agent changed the crystallization characteristics of the composites. This along with enhanced filler−matrix interaction resulted in an increase in flexural strength and modulus in RFAPA1 and RFAPA2 with respect to RFAPA0. The impact strength increased significantly by 132% in RFAPA1 compared to that of RFAPA0. In DMA analysis, the highest increase in storage modulus was found in RFAPA1, with a shift in glass transition temperature to higher values in both RFAPA1 and RFAPA2. Enhanced filler−matrix interaction at the interface in the presence of a PA coupling agent also resulted in increased thermal stability of the composites as evidenced from TGA. DSC analysis also revealed that incorporation of filler influenced their crystalline characteristics leading to changes in their thermal properties. A more compatibilized interface was visible in PA-coated FA/R composites from the SEM analysis.

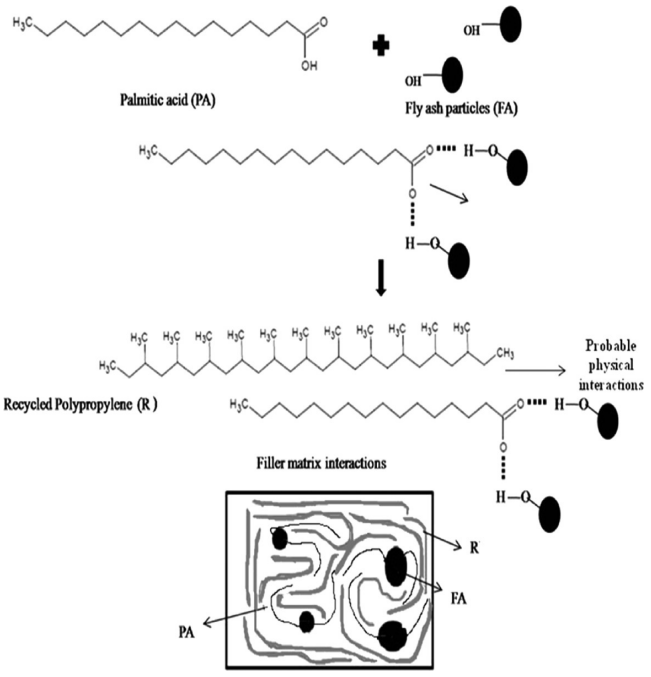

Figure 8. Schematic representation of the filler−matrix interaction in PA-coated FA/R composites depicting a probable physical interaction and correlating the filler−matrix compatibility with the observed SEM micrographs.

This study therefore shows the possibility of using a green renewable chemical like palmitic acid as a coupling agent in FA/R composites, especially in 1 and 2 wt % concentration to achieve high-performance tailor-made composites, withstanding service conditions. Thus, palmitic acid-coated fly ash-reinforced R composites could be developed as economically viable sustainable materials having good mechanical strength and thermal stability.

AUTHOR INFORMATION

Corresponding Author

*Tel.: +91 033 2350 1397. Fax: +91 033 2351 9755. E-mails: roy.dipa@gmail.com.

Notes

The authors declare no competing financial interest.

ACKNOWLEDGMENTS

Shubhalakshmi Sengupta is thankful to the Department of Science and Technology (DST), Government of India, for her fellowship. Dipa Ray is thankful to DST, Government of India, for granting her the project. The authors are thankful to N. R. Bandyopadhyay, Malay Kundu, and Arpita Jana of the School of Materials Science and Engineering, BESUS, India, for their help in flexural testing and SEM analysis.

REFERENCES

(1) Parvaiz, M. R.; Mahanawar, P. A.; Mohanty, S.; Nayak, S. K. Effect of surface modification of fly ash reinforced in polyether-etherketone composites. *Polym. Compos.* **2011**, *32*, 1115−1124.

(2) Iraola-Arregui, I.; Potgieter, H.; Liauw, C. M. Evaluation of coupling agents in poly (propylene)/fly ash composites: Effect on processing and mechanical properties. *Macromol. Mater. Eng.* **2011**, *296*, 810−819.

(3) Ma, X. F.; Yu, J. G.; Wang, N. Fly ash reinforced thermoplastic starch composites. *Carbohydr. Polym.* **2007**, *67*, 32−39.

(4) Pardo, S. G.; Bernat, C.; Abad, M. J.; Caro, J. Rheological, thermal and mechanical characterization of fly ash-thermoplastic composites with different coupling agents. *Polym. Compos.* **2010**, *31*, 1722−1730.

(5) Ray, D.; Bhattacharya, D.; Mohanty, A. K.; Drzal, L. T.; Misra, M. Static and dynamic mechanical properties of vinylester resin matrix composites filled with fly ash. *Macromol. Mater. Eng.* **2006**, *291*, 784−792.

(6) Guhanathan, S.; Sarojadevi, M. Studies on interface in polystyrene/fly ash particulate composites. *Comp. Interface.* **2004**, *11*, 43−66.

(7) Sridhar, V.; Xiu, Z. Z.; Xu, D.; Lee, S. H.; Kim, J. K.; Kang, D. J.; Bang, D. Fly ash reinforced thermoplastic vulcanizates from waste tire powder. *Waste Manage.* **2009**, *29*, 1058−1066.

(8) Nath, D. C. D.; Bandyopadhyay, S.; Yu, A.; Blackburn, D.; White, C. High strength bio-composite films of poly (vinyl alcohol) reinforced with chemically modified fly ash. *J. Mater. Sci.* **2010**, *45*, 1354−1360.

(9) Gupta, N.; Brar, B. S.; Woldesenbet, E. Effects of filler addition on the compressive and impact properties of glass fibre reinforced epoxy. *Bull. Mater. Sci.* **2001**, *24*, 219−223.

(10) Menon, A. R. R.; Sonia, T. A.; Sudha, J. D. Studies on fly ash-filled natural rubber modified with cardanol derivatives: Processability, mechanical properties, fracture morphology and thermal decomposition characteristics. *J. Appl. Polym. Sci.* **2006**, *102*, 4801−4808.

(11) Ray, D.; Banerjee, S.; Mohanty, A. K.; Misra, M. Thermal and electrical behaviour of vinylester resin matrix composites filled with fly ash particles. *Polym. Compos.* **2008**, *29*, 58−62.

(12) Yu-fen, Y.; Guo-Shen, G.; Zhen-Fang, C.; Qing-Ru, C. Surface modification of purified fly ash and application in polymer. *J. Hazard. Mater.* **2000**, *B133*, 276−282.

(13) Bose, S.; Mahanwar, P. A. Effect of titanate coupling agent on the mechanical, thermal, dielectric, rheological, and morphological properties of filled nylon 6. *J. Appl. Polym. Sci.* **2006**, *99*, 266−272.

(14) Nath, D. C. D.; Bandyopadhyay, S.; Gupta, S.; Yu, A.; Blackburn, D.; White, C. Surface- coated fly ash used as filler in biodegradable poly (vinyl alcohol) composite films: Part 1.The modification process. *Appl. Surf. Sci.* **2010**, *256*, 2759−2763.

(15) Das, K.; Ray, D.; Adhikary, K.; Bandyopadhyay, N. R.; Mohanty, A. K.; Misra, M. Development of recycled polypropylene matrix composites reinforced with fly ash. *J. Reinf. Plast. Compos.* **2009**, *29*, 510−517.

(16) Sengupta, S.; Pal, K.; Ray, D.; Mukhopadhyay, A. Furfuryl palmitate coated fly ash used as filler in recycled polypropylene matrix composites. *Composites, Part B.* **2011**, *42*, 1834−1839.

(17) Nath, D. C. D.; Bandyopadhyay, S.; Yu, A.; Zeng, Q.; Das, T.; Blackburn, D.; White, C. Structure−property interface correlation of fly ash: Isotactic polypropylene composites. *J. Mater. Sci.* **2009**, *44*, 6078−6089.

(18) ASTM D790-10 Standard Test Methods for Flexural Properties of Unreinforced and Reinforced Plastics and Electrical Insulating Materials. http://enterprise.astm.org/filtrexx40.cgi?+REDLINE_PAGES/D790.htm (accessed May 3, 2013).

(19) ASTM D256-10 Standard Test Methods for Determining the Izod Pendulum Impact Resistance of Plastics. http://enterprise.astm.org/filtrexx40.cgi?+REDLINE_PAGES/D256.htm (accessed May 3, 2013).

(20) Sengupta, S.; Maity, P.; Ray, D.; Mukhopadhyay, A. Thermal and structural characterization of furfuryl palmitate coated fly ash reinforced recycled polypropylenematrix composites. *Adv. Mater. Res.* **2012**, *584*, 551−556.

(21) Das, K.; Ray, D.; Bandyopadhyay, N. R.; Sengupta, S. Study of the properties of microcrystalline cellulose particles from different renewable resources by XRD, FTIR, nanoindentation, TGA and SEM. *J. Polym. Environ.* **2010**, *18*, 355−363.

(22) Tortorella, N.; Beatty, C. L. Morphology and crystalline properties of impact modified polypropylene blends. *Polym. Eng. Sci.* **2008**, *48*, 1476−1486.

(23) Satpathy, B. K.; Das, A.; Patnaik, A. Ductile-to-brittle transition in cenosphere-filled polypropylene composites. *J. Mater. Sci.* **2011**, *46*, 1963−1974.
(24) Bhattacharya, A. R.; Sreekumar, T. V.; Liu, T.; Kumar, S.; Ericson, L. M.; Hauge, R. H.; Smalley, R. E. Crystallization and orientation studies in in polypropylene/SWNT composites. *Polymer* **2003**, *44*, 2373−2377.
(25) Ray, D.; Sengupta, S.; Sengupta, S. P.; Mohanty, A. K.; Misra, M. Preparation and properties of vinylester resin/clay nanocomposites. *Macromol. Mater. Eng.* **2006**, *291*, 1513−1520.
(26) Mustapa, M. S. E.; Hassan, A.; Rahmat, R. R. Preliminary Study on the Mechanical Properties of PP Rice Husk Composites. In *Proceedings of Simposium Polymer Kebangsaan Ke-V Hotel Residence*, August 2005, Universiti Teknologi Malaysia Institutional Repository. http://eprints.utm.my/3267/1/L14_spk05_fp_Mohd_Shahril.pdf
(27) Feng, D.; Caulfield, F.; Sanadi, A. R. Effect of compatibilizer on the structure−property relationships of kenaf−fiber/polypropylene composites. *Polym. Compos.* **2001**, *22*, 506−517.